

Large-scale coherent structures in the wake of axisymmetric bodies

By H. V. FUCHS,†

DFVLR-Institut für Turbulenzforschung, 1000 Berlin 12

E. MERCKER

Hermann-Föttinger-Institut für Thermo- und Fluidodynamik,
Technische Universität, 1000 Berlin 12

AND U. MICHEL

DFVLR-Institut für Turbulenzforschung, 1000 Berlin 12

(Received 14 August 1978)

The unsteady flow past a circular disk is studied with hot-wire and microphone probes positioned in planes normal to the axis of symmetry at 3 and 9 disk diameters downstream. Both the fluctuating velocity and pressure signals are shown to be continuously dominated by large-scale coherent motions enveloping the wake flow as a whole. This suggests narrowband two-point space correlations as an experimental tool for describing spatial coherence and phase characteristics of the basically random signals. The specific symmetry imposed by the axisymmetric boundary conditions of the disk enables a decomposition of the large-scale flow phenomena into relatively simple elementary structures or modes. The resulting azimuthal constituents are quantified in terms of their respective magnitudes and individual power spectra.

The capability of the approach to uncover characteristic features of turbulence as far as its large-scale domain is concerned is demonstrated by a comparison of the present results with certain remarkably different features found in earlier jet flow investigations: the $m = 1$ and $m = 2$ modes are found to clearly dominate in wakes whereas the $m = 0$ and $m = 1$ modes were dominant in jets in a relevant range of Strouhal numbers. These large-scale coherent structures are more than just an interesting flow phenomenon; they must have a tremendous back-reaction on rigid flow boundaries (particularly if these allow a vibrational response) and may give rise to specific feedback mechanisms.

The analysing technique proposed for studying large-scale flow phenomena in jets and wakes removes part of the randomness in the turbulent signals without artificially exciting or forcing them in one way or another. No conditional sampling of the naturally occurring fluctuations is required, either. The method may be applicable to other than strictly axisymmetric flow configurations, too.

1. Introduction

Turbulence research is often concerned with measuring the intensities, power spectra and covariances of random properties (usually velocities) in the flow under investigation. One objective of these single-point measurements is to study the effect

† Present address: FhG-Institut für Bauphysik, 7000 Stuttgart 700.

of turbulence on the mean flow behaviour *via* some form of Reynolds' equations. Mixing length or eddy models are sometimes adopted by analogy with the kinetic theory of gases. Typical eddy scales l and convection velocities U_c can be determined from conventional space-time correlation measurements.

In contrast to the molecular motion in gases, however, there is also the possibility of a turbulent motion at one point of a continuous fluid flow influencing the simultaneous motion at another distant point. This weakly coherent turbulent motion, though more organized than molecular motion on a microscale, may still appear as completely random on the mean flow scale L with $l \ll L$ defining what is usually termed 'small scale turbulence'. It is to such random fields that statistical descriptions are fully applicable and quasi-local averaging procedures adequate.

If, at least, part of the turbulent motion is found to be coherent over distances of the order L our standard description of turbulence, much of which was guided by the idealized theoretical concept of isotropic turbulence, becomes less appropriate. When dealing with 'large-scale turbulence' one is forced to look at the unsteady flow field as a whole and simultaneously. Turbulent motions of this kind represent themselves as characteristic *structures* which dominate the flow rather than as local perturbations of a pre-existing mean motion. Due to their dominating both the steady and unsteady flow field these large-scale turbulent structures are intimately tied up with the geometrical and symmetry conditions imposed on the flow by its boundaries, e.g. of the nozzle in the case of a free jet or of the body in the case of a wake flow.

The large-scale structures, which will be described in more detail in the ensuing sections, bear some faint resemblance to Townsend's (1956) 'large eddies' which are thought to arise spontaneously as a chance configuration of the small-scale eddies. In this model it is still the small-scale eddies that contribute most to the locally measurable mean-square turbulence energy. Townsend's hypothesis of randomly occurring chance eddies led Grant (1958) to define physical models of 'typical eddies' in two-dimensional turbulent wake and boundary-layer flows on the basis of the following.

- (1) The eddies are of a size much larger than any other component of the turbulence.
- (2) The eddies are placed at random in the x, y plane.
- (3) The motions of adjacent or overlapping eddies are statistically independent.

From the nine velocity correlations $R_{ii}(r_j)$ measured Grant postulated 'vortex pair eddies' with their axes in the x, y plane and with opposite circulations in the x, z plane of the cylinder wake. For the boundary layer Grant postulated 'mixing jets' with velocities mainly in the x, y plane to fit his correlation curves. His idea of sudden outward eruptions of fluid from the laminar sublayer near the wall into the turbulent region prompted a number of researchers to hunt and pin down such figurative phenomena as 'bursts', 'spots', 'sweeps', 'slugs', 'puffs', 'bulges', or even more illustrative 'buffaloes' and 'tornadoes'.

According to Townsend's model, initiation of any type of large eddies is by mere coincidence or alignment of small eddies rather than by a natural tendency towards order of the unsteady flow as one coherent entity. Special detection schemes employing conditional ensemble averaging (see, e.g. Kovasznay, Kibens & Blackwelder 1970) and sophisticated pattern-recognition methods were already invented in order to explore these new statistical phenomena.

The present paper deals with turbulent structures in a distinctly different way

which was initially stimulated by *narrowband*, unconditioned two-point correlation measurements of Fuchs (1972) performed in the turbulent pressure field of a circular jet. These revealed a very regular, well-ordered turbulence pattern travelling in the central mixing region in an almost deterministic *wave-like* manner. By contrast to the highly intermittent character of the turbulent features described above, large-scale structures as we see them are more or less continuously present in the flow. They are absolutely predominant in the turbulent signal at e.g. a fluctuating pressure or velocity probe inserted in a jet flow.

The last mentioned coherent structures could be shown by Armstrong, Michalke & Fuchs (1977) to exist in a wide range of jet Mach and Reynolds numbers, namely $0.1 < Ma < 0.7$, $10^4 < Re < 10^6$. In fact, no method so far known will prevent their occurrence in the axial range $1 < x/D < 12$. These structures should therefore not be confused with those that can be artificially excited by internal or external disturbances acting on the flow. It is also pointed out that an ordinary cross spectral analysis is fully sufficient for studying these structures with no conditional sampling technique being required.

2. A quantitative description of turbulent structures

Ever since Townsend (1956) put forward his 'big eddies' idea attempts were made to condense more than just vague qualitative information on typical eddy structures from the shape of measured two-point correlation functions of the turbulent velocity field. None of these efforts, however, has enabled a strictly quantitative analysis. Most of our own previous work on turbulence structures lies buried in the jungles of jet noise literature (refer e.g. to Michalke & Fuchs 1975). It seems to have passed largely unnoticed by the fluid dynamicists proper. Our approach is fairly fundamental and almost universally applicable, although its specific virtue could, up till now, only be demonstrated for axisymmetric free shear flows.

Given an arbitrary space correlation function $R(r_i)$ of a turbulent field quantity, say $p(t)$, we may straightforwardly define its Fourier transform in any one of the three dimensions of displacement r_i ,

$$F(k_i) = \int_V R(r_i) \exp(ik_j r_j) dr_i. \quad (1)$$

The resulting complex wavenumber spectrum $F(k_i)$ should not be confused with frequency spectra $F(\omega)$ from Fourier transforms in the time domain. R may, however, represent the correlation C_ω of a narrowband frequency component $p_\omega(t)$.

For illustrative purposes we may consider the one-dimensional transform under two very special conditions (figure 1),

(1) R be a *real* function of the displacement r , $R^*(r) = R(r)$.

(2) R be *symmetric* in r , $R(-r) = R(r)$.

It is pointed out that r need not be in the direction of the mean flow and hence k in

$$F(k) = 2 \int_0^\infty R(r) \cos kr dr \quad (2)$$

is not necessarily associated with any kind of wave propagation or convection of disturbances with the mean flow.

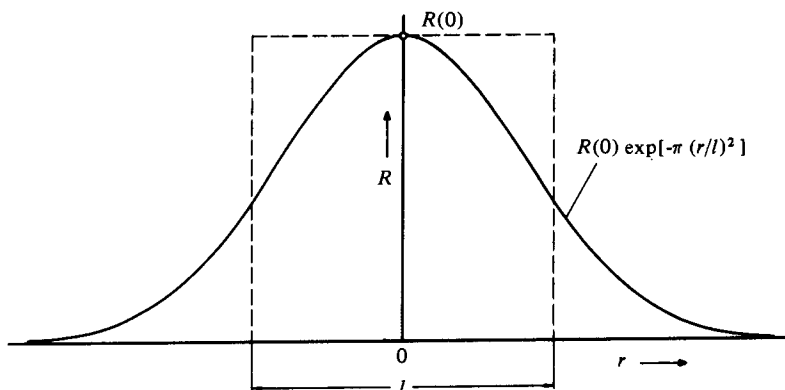


FIGURE 1. Idealized two-point space correlation in small-scale isotropic turbulence. l = integral length scale or eddy size.

It is only the most trivial case $k = 0$ that is frequently called upon when a random turbulent field is to be characterized,

$$F(0) = 2 \int_0^{\infty} R(r) dr \quad (3)$$

with

$$l = \frac{F(0)}{R(0)} = 2 \int_0^{\infty} \frac{R(r)}{R(0)} dr \quad (4)$$

defining the scale or size of an average eddy. If, for instance, $R(r)$ always had a Gaussian form,

$$R(r) = R(0) \exp[-\pi(r/l)^2], \quad (5)$$

l would indeed suffice to completely characterize the turbulent field. Under more general circumstances, however, where $R(r)$ may exhibit one or more zero crossings, l does not seem to be a very significant parameter to be determined.

Several ideas are currently ventilated in our group how to make use of the full wavenumber spectrum $F(k)$ when large-scale turbulent structures are to be described. Potential applications lie in two-dimensional ($2d$) flow configurations with certain boundary conditions on which we cannot elaborate here.

Our approach seems particularly attractive and has, in fact, already proved to be a very handy tool as far as axisymmetric free shear layers are concerned. Before we proceed to the practically important jet and wake flows, we remind ourselves that, for any approach *via* ordinary long time averages $R(r)$ to be successful, it is essential to have the structures *continuously dominate* the unsteady flow field. The well-correlated portion of $p(t)$ would otherwise be degraded by the other contributions to the total turbulent signal. We note that we are interested only in *self-generated*, i.e. not externally driven disturbances. The turbulent signals will hence always remain basically random in time.

Under these fairly general conditions a maximum of useful information about the space-time structure of a turbulent field can be extracted from the complex two-point cross-spectral density function

$$R_{\omega} = C_{\omega} + iQ_{\omega}, \quad (6)$$

where both the coincident and the quadrature spectra, C_{ω} and Q_{ω} , may be functions of the moving as well as of the fixed probe positions, indices 2 and 1. For a most

convenient description of the coherent phenomena in turbulence the total information is suitably subdivided into three categories according to the following expression,

$$R_\omega = \tilde{p}_{\omega,1} \tilde{p}_{\omega,2} \frac{|R_\omega|}{\tilde{p}_{\omega,1} \tilde{p}_{\omega,2}} \exp i\psi_\omega, \quad (7)$$

with

(A) $\tilde{p}_\omega = \overline{(p_\omega^2)}^{\frac{1}{2}}$ denoting the local power spectral density, or *strength*, of the turbulent property measured,

(B) $\gamma = |R_\omega|/(\tilde{p}_{\omega,1} \tilde{p}_{\omega,2}) = (C_\omega^2 + Q_\omega^2)^{\frac{1}{2}}/(\tilde{p}_{\omega,1} \tilde{p}_{\omega,2})$ denoting the degree of statistical correlation, or *coherence*, of signals at two distant points in the flow,

(C) $\psi_\omega = \overline{\psi_{\omega,2}} - \overline{\psi_{\omega,1}}$ denoting an averaged *phase* relationship between both signals.

Category (A) is normally dealt with in conventional turbulence studies with \tilde{p}_ω or \tilde{p} suitably normalized with the appropriate mean flow properties. Category (C) contains all the information concerning the convection of disturbances by the flow. In this paper we shall focus our attention on mainly the coherence properties and restrict our analysis to a specific class of flow configurations.

3. The azimuthal constituents of turbulence in axisymmetric flows

Strictly axisymmetric flow conditions allow three very decisive assumptions to be made. If, to start with, both probes are located on a constant radius r in a plane $x = \text{const.}$ normal to the axis of symmetry one may easily convince oneself that, for circumferential displacements $\Delta\phi$,

(1) Q_ω is identically zero within experimental error provided that no mean swirl is superimposed on the flow, i.e. there is no preferred helical propagation for the disturbances while travelling downstream so that $\psi_\omega = \tan^{-1} Q_\omega/C_\omega = 0$. Hence we are dealing with the *real* function $R_\omega = C_\omega = R_\omega^*$.

(2) For similar symmetry reasons, C_ω is *symmetric* in $\Delta\phi$, i.e. $C_\omega(-\Delta\phi) = C_\omega(\Delta\phi)$.

(3) The most important feature of axisymmetric flows, however, is the spatial *periodicity* inherent in circumferential correlation functions at any arbitrary radius, $C_\omega(\Delta\phi + n2\pi) = C_\omega(\Delta\phi)$.

Under these very special conditions the Fourier integral (2) can be replaced by a much simpler expression,

$$F = C_{\omega,m} = \frac{1}{\pi} \int_0^\pi C_\omega(\Delta\phi) \cos m\Delta\phi d\phi, \quad (2a)$$

with $C_{\omega,m}$ defining the discrete coefficients in a Fourier *series* of C_ω ,

$$C_\omega(\Delta\phi) = \sum_{m=0}^m C_{\omega,m} \cos m\Delta\phi. \quad (8)$$

With its value at $\Delta\phi = 0$,

$$C_\omega(0) = \sum_{m=0}^\infty C_{\omega,m} = \overline{p_\omega^2} = \sum_{m=0}^\infty \overline{p_{\omega,m}^2}, \quad (9)$$

it is made possible to define the fraction of fluctuating energy contained in each individual azimuthal constituent of order m by

$$\frac{\overline{p_{\omega,m}^2}}{\overline{p_\omega^2}} = \frac{C_{\omega,m}}{C_\omega(0)}. \quad (10)$$

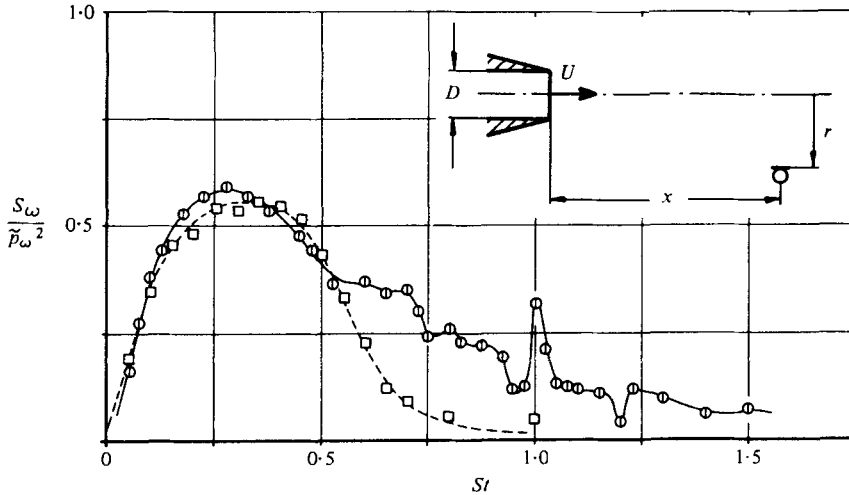


FIGURE 2. Coherence spectrum of turbulent pressure fluctuations near circular jet flows from Fuchs & Michel (1977). $\Delta\phi = 60^\circ$. - - - - , model jet at $x = 6D$, $r = 1.5D$, $Ma = 0.3$; —, jet engine at $x = 5D$, $r = 1.4D$, $Ma = 0.52$.

Co-spectra C_ω are readily obtained with the aid of a digital computer by using a Fast Fourier Transform routine thus enabling several different kinds of representation of turbulence structure.

(a) The first is based on the *spatial coherence* of the turbulent quantity as defined in equation (7) which, in this special case, with $\tilde{p}_{\omega,2} = \tilde{p}_{\omega,1} = \tilde{p}_\omega$ would read

$$\gamma = \frac{S_\omega}{\tilde{p}_\omega^2} \equiv \frac{|R_\omega|}{\tilde{p}_\omega^2} = \frac{|C_\omega|}{\tilde{p}_\omega^2} = f(St); \quad \Delta\phi = \text{const.} \tag{11}$$

With γ varying between 0 and 1, it normally represents a measure of how coherent two turbulent signals are. Its magnitude usually exceeds the absolute value of corresponding broadband correlation coefficients $R_{12}/\tilde{p}_1\tilde{p}_2$ and hence may help to detect large-scale coherent motions where ordinary correlation analyses fail. The variation of γ with frequency also shows at what frequencies coherent structures are present or strongest. To illustrate this, figure 2 exhibits the coherence of turbulent pressure fluctuations $p(t)$ in the near field close to a circular model jet and a real jet engine at geometrically similar points. Coherence peaks at a typical frequency or better Strouhal number $St = fD/U$ ($f =$ frequency, $D =$ nozzle diameter, $U =$ exit velocity) around 0.3 whereas the corresponding power spectra \tilde{p}_ω^2 at that position peak at much lower St . Plotting coherence spectra, however, does not yet tell us very much about the specific character of the coherent motions involved in any particular flow.

(b) We can gain more insight into the structures responsible for the high coherence observed in the jet pressure field by picking a narrowband component C_ω preferably in that narrow range of frequencies where the coherence is strongest and look at its *variation with $\Delta\phi$* at the circumference of the jet. Figure 3 shows a plot of

$$C_\omega/\tilde{p}_\omega^2 = f(\Delta\phi); \quad St = \text{const.} \tag{12}$$

right in the middle of the mixing region of a circular jet ($r = 0.5D$). The very moderate fall of the correlation with increasing probe displacement is characteristic of the jet

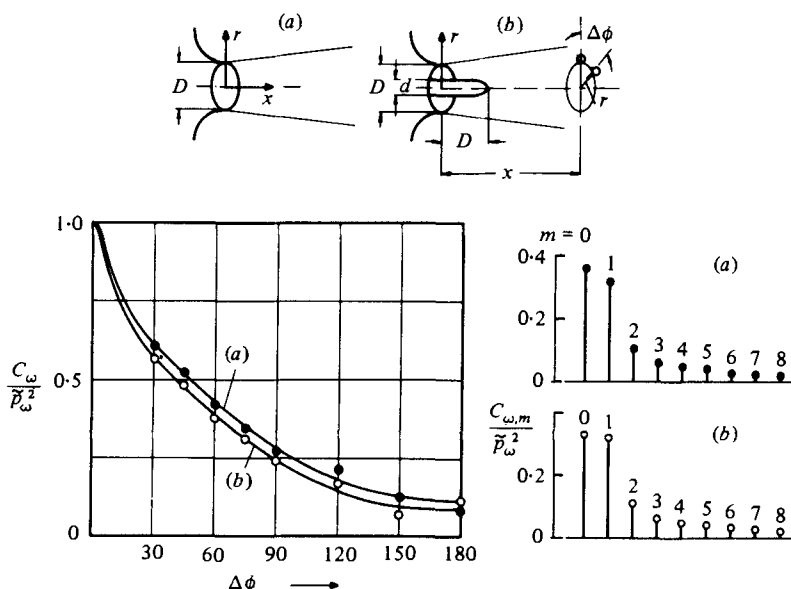


FIGURE 3. Circumferential correlation of a narrowband component of the turbulent pressure field inside the mixing region of a model jet (a) without and (b) with an axisymmetric centre body according to Michel & Fuchs (1978). $d/D = 0.4$, $x = 3D$, $r = 0.5D$, $Ma = 0.15$, $St = 0.45$. Right: corresponding azimuthal constituents.

pressure field. Similar circumferential correlations in wake flows will later be seen to exhibit completely different curves over $\Delta\phi$ thus indicating, if only qualitatively, significant differences in the respective turbulent structures involved.

(c) The last assertion of correlations uncovering the nature of large-scale structures can be converted into a *strictly quantitative* analysis by displaying the strength of the individual *azimuthal constituents*, $\bar{p}_{\omega,m}^2$, in proportion to the overall, i.e. unresolved quantity \bar{p}_{ω}^2 according to equation (10),

$$C_{\omega,m}/\bar{p}_{\omega}^2 = f(m); \quad St = \text{const.} \quad (13)$$

The result of such a Fourier analysis is also depicted in figure 3. The extraordinary dominance of the $m = 0$ and $m = 1$ constituents must be regarded as a characteristic feature of the early development well into the transition region of a turbulent jet. It is not easily affected by internal or external disturbances as may be seen by comparison with case (b) when an axisymmetric centre body is introduced through the nozzle.

The $m = 0$ constituent is characterized by an in-phase relationship of signals p_1 and p_2 detected simultaneously by probes facing each other across the jet whereas the $m = 1$ mode is due to signals in anti-phase. Using $p_1 + p_2$ or $p_1 - p_2$ signals thus enables discrimination of one mode against the other as was demonstrated by Fuchs (1973). Moore (1977) made use of a similar trick when he, very successfully, visualized the two modes separately by multiple-exposure flash photographs triggered with large signals $p_1 + p_2$ or $p_1 - p_2$, respectively (see Moore's plate 5).

The above described Fourier expansion of turbulent structures is particularly useful whenever we find a small number of modes prevailing. Needless to say that it is not restricted to the instantaneous or time averaged value of a turbulent quantity

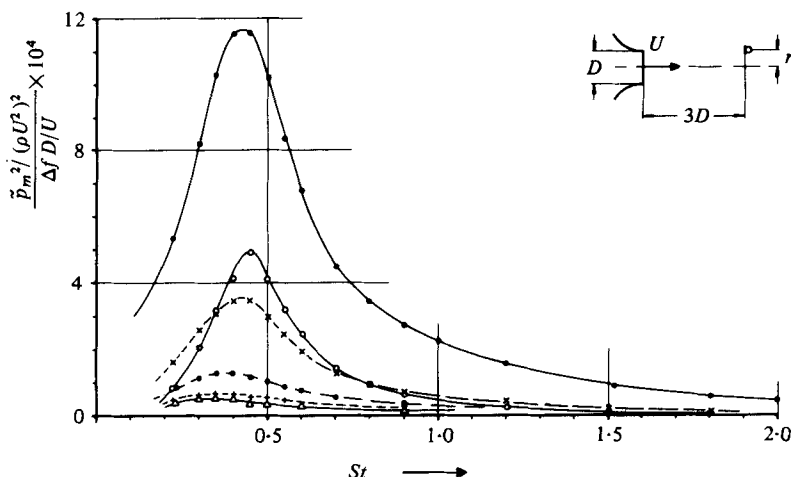


FIGURE 4. Normalized power spectra of azimuthal constituents of jet pressure at $x = 3D$, $r = 0.5D$ from Michalke & Fuchs (1975). —, normalized overall (unresolved) power spectrum; \bigcirc — \bigcirc , $m = 0$; \times — \times , $m = 1$; \bullet — \bullet , $m = 2$; $+$ — $+$, $m = 3$; Δ — Δ , $m = 4$.

at a constant axial and radial position. In calculating noise generated by turbulence e.g., one has to deal with more general two-point correlations and hence to resolve both C_ω and Q_ω or S_ω correspondingly (refer to Armstrong *et al.* 1977).

(d) In many applications one may be interested in not only the coherence of a turbulent field and the strength of the different structures relative to one another (representations (11) through (13)), but also in suitably *normalized power spectra* of the azimuthal constituents individually,

$$\frac{\tilde{p}_m^2 / (\rho U^2)^2}{\Delta f D / U} = \frac{\tilde{p}_{\omega, m}^2 / (\rho U^2)^2}{D / U} = f(St). \quad (14)$$

Herein \tilde{p}_m^2 is the mean square of mode m in the measuring bandwidth Δf chosen. A typical such plot is shown as figure 4 for the circular jet.

For a complete mapping of a highly inhomogeneous and non-isotropic turbulent field one would, of course, need to also plot the spatial variations of all the representations discussed above.

4. Mean and mean-square characteristics of the flow past a circular disk

The main objective of this paper is to describe characteristic features of the turbulence in axisymmetric wakes as compared to that in axisymmetric jets. Our approach is novel only as far as the interpretation of two-point cross correlation functions is concerned. To this end, the structure of the mean flow in which the measurements are done is irrelevant. Likewise, the intensity or strength of the turbulent fluctuations the geometrical structures of which are to be described, are of secondary importance. We have therefore decided to discuss the more conventional single-point measurements with respect to similar data published in the relevant literature in a separate paper by Fuchs, Mercker & Michel (to be published).

It may suffice here to report that all our experiments were performed with axi-

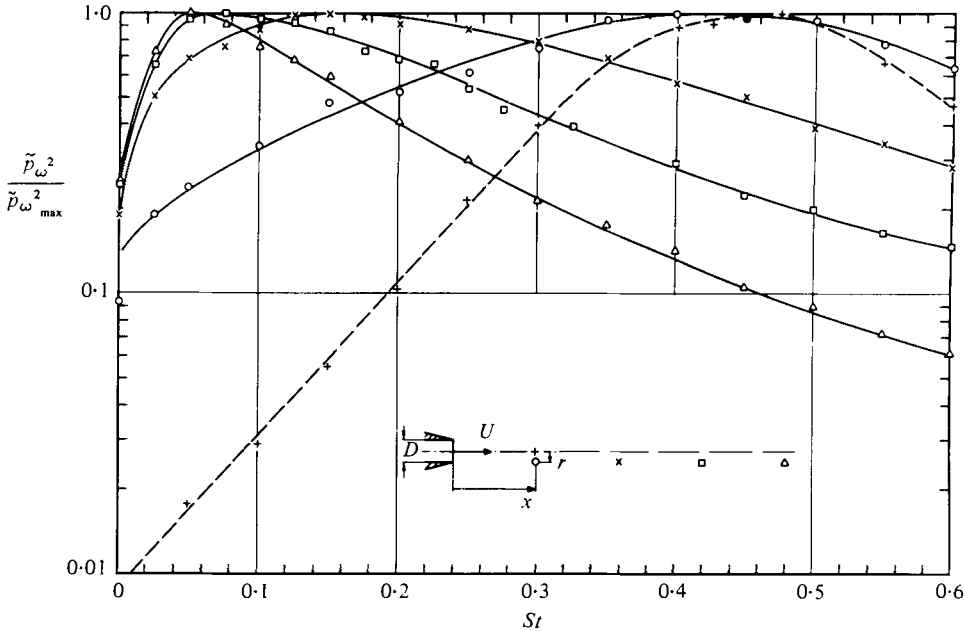


FIGURE 5. Shape of power spectra of turbulent jet pressure fluctuations at various downstream positions (unpublished data by R. R. Armstrong). $Ma = 0.3$, $Re = 7 \times 10^5$; $r = 0.5D$: \circ , $x = 3D$; \times , $x = 6D$; \square , $x = 9D$; \triangle , $x = 12D$. $r = 0$; $+$, $x = 3D$.

symmetric bodies (a disk and a 120° cone), $D = 50$ mm in diameter, mounted normal to the flow in an open jet wind tunnel of 1 m diameter. The Reynolds number as based on D was held constant at about 5×10^4 , a value typical of most of the previous experiments. The downstream stagnation point e.g. was $x = 2.5D$ downstream from the disk. It marked the region where the root-mean-square (r.m.s.) pressure \tilde{p} reaches its maximum of nearly 12% of the total head $0.5\rho U^2$. The pressure signals from two B & K condenser microphone probes ($\frac{1}{8}$ in.) fitted with nose cones seem not to have been contaminated too badly by acoustic or turbulent background noise at least in the measuring plane $x = 3D$. At $x = 9D$, where $\tilde{p}_\omega/0.5\rho U^2$ hardly exceeded 0.03, the pressure signals could not be related to the turbulence structure of the wake and hence measurements in that plane were restricted to the streamwise velocity fluctuations from linearized constant temperature hot-wire anemometers.

5. Quasi-periodic wake phenomena

Free jet turbulence was chosen first for illustrating the usefulness of our quantitative approach to large-scale structures. Figure 4 showed that the dominance of only a few lower order constituents is restricted to a fairly narrow range of Strouhal numbers with their respective power spectra \tilde{p}_m^2 peaking at almost exactly the same frequency as \tilde{p}_ω^2 , the overall (unresolved) power spectrum. This spectral peak is seen in figure 5 to vary considerably with downstream position. According to Laufer, Kaplan & Chu (1973), the coalescence and pairing of two or more adjacent vortices is responsible for this apparently reversed cascade process whereby smaller scales or wavelengths are continuously converted into larger scales while travelling downstream. It is

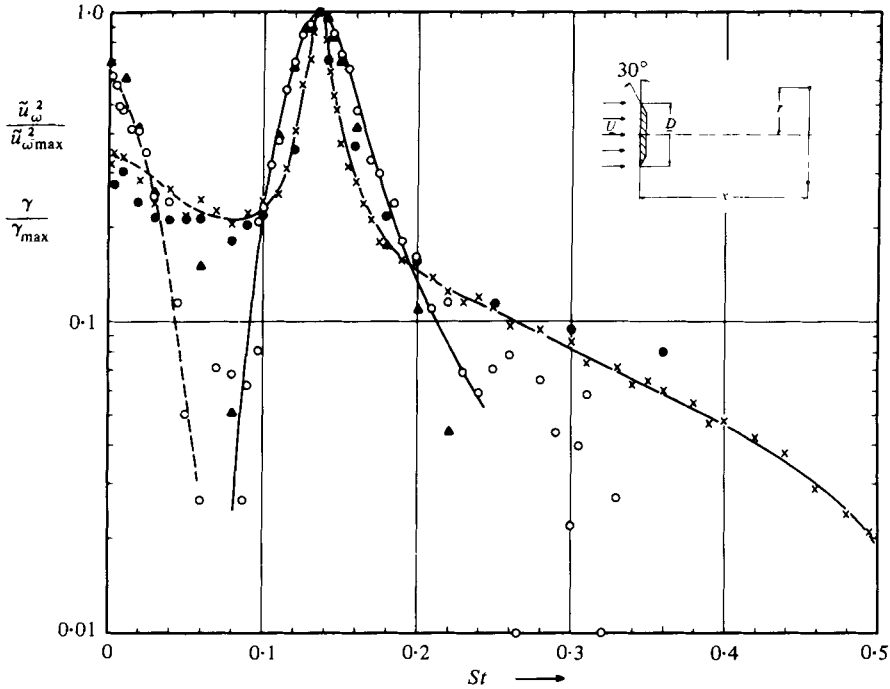


FIGURE 6. Shape of power spectra and coherence spectra of streamwise velocity fluctuations in the wake of a circular disk. $D = 50$ mm, $U = 15$ m/s. \times , power spectrum at $x = 9D$, $r = 0.83D$; \bullet , Roberts' (1973) data; \circ , coherence spectrum, $\Delta\phi = 180^\circ$; \blacktriangle , Roberts' (1973) data.

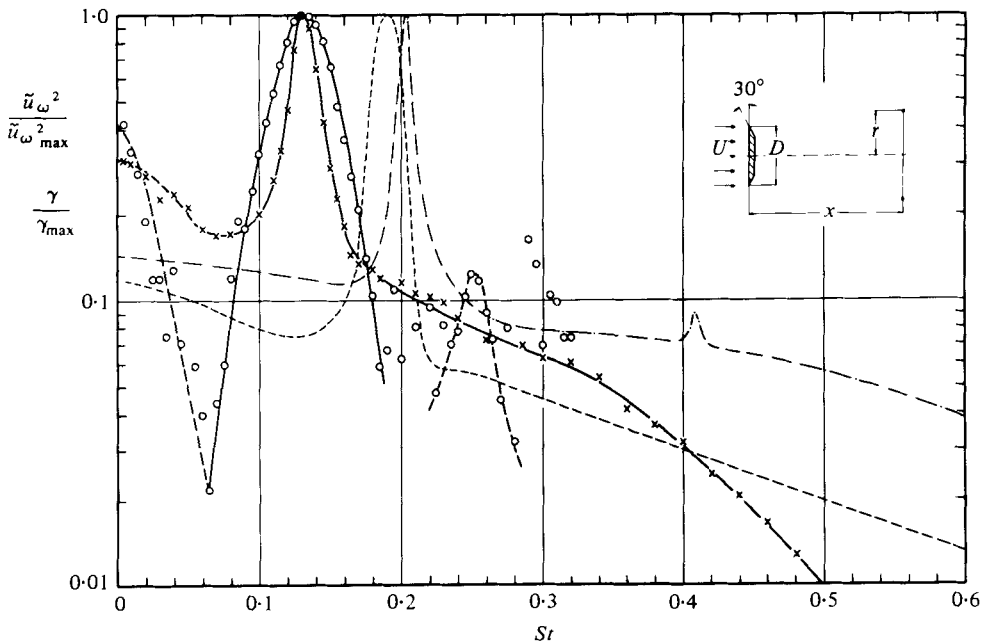


FIGURE 7. Shape of power spectra and coherence spectra of streamwise velocity fluctuations in wakes. $Re = 5 \times 10^4$. \times , power spectrum at $x = 3D$, $r = 0.75D$; \circ , coherence spectrum, $\Delta\phi = 180^\circ$; ---, cylinder wake power spectrum by Surry & Surry (1967), $x = 7.45D$, $r = 0.38D$; —, triangular cylinder wake power spectrum by Mercker & Fiedler (1978), $x = 3D$, $r = 1.5D$.

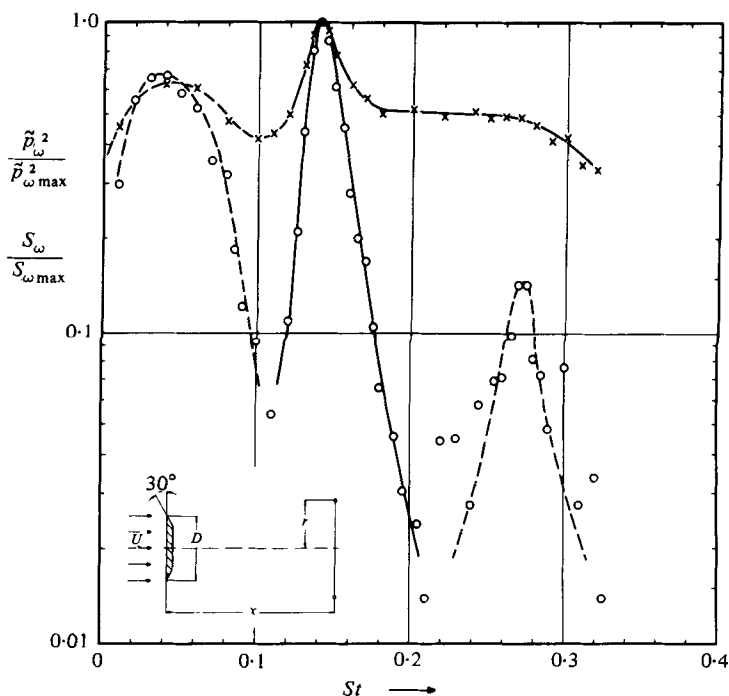


FIGURE 8. Shape of power spectrum and cross spectrum of pressure fluctuations in disk wake at $x = 3D$, $r = 0.75D$; \times , power spectrum; \circ , cross spectrum, $\Delta\phi = 180^\circ$.

recalled, however, that modelling the turbulence by annular vortex rings, i.e. by merely the $m = 0$ mode, is surely an oversimplified picture of the large structures in a jet. It would be equally misleading if one thought of the coherent motions as simple travelling waves with a periodicity induced, once for all, by the vortex shedding at the nozzle lip.

That view of a regular vortex street is more appropriate when dealing with the large structures in wake flows. The non-dimensional velocity power spectra,

$$\hat{u}_\omega^2 / \hat{u}_{\omega\max}^2 = f(St), \quad (15)$$

in figures 6 and 7 have maxima around $St_0 = 0.135$ which are considerably narrower than those of the jet pressure spectra (figure 5) and with St_0 hardly varying at all between $x = 3D$ and $9D$. The shape of the spectrum measured at $x = 9D$ compares favourably with Roberts' (1973) data (full circles in figure 6) obtained at a Reynolds number 7.8×10^4 as compared to 5×10^4 in our experiments. It may be noted that these spectra look very much the same as those in the wake of circular or triangular cylinders in a cross flow. The dashed curves in figure 7 represent the results of Surry & Surry (1967) at $Re = 2.6 \times 10^4$ and of Mercker & Fiedler (1978) at $Re = 5.2 \times 10^4$. Surry & Surry also report a decrease in the ratio of the peak height to the height of the underlying 'base' spectrum with increasing x/d with the peak frequency itself remaining constant in accordance with our disk results.

The *periodicity* around $St_0 = 0.135$ is also visible in the fluctuating pressure at $x = 3D$ (figure 8). These spectral analyses suggest that underlying the apparent chaos in axisymmetric wakes, there may be a well-ordered turbulence structure of a similar

nature as in a Kármán vortex sheet. A possible reason for their not having been observed in the past may be that the anti-symmetric structure which so obviously dominates the vortex street in a plane normal to the cylinder does not find a similarly predetermined orientation in the wake of an axisymmetric body as it does in the cylinder wake. While the resulting randomness will presumably render visualizations of the structures as difficult as in a round jet, it leaves our quantitative approach entirely unaffected since this is based on straightforward long time averaged covariance measurements.

6. Coherence spectra in the axisymmetric wake

We commenced our analysis of axisymmetric wake turbulence by determining its coherence γ according to equation (11) as a function of St . For measuring positions facing each other across the wake ($\Delta\phi = 180^\circ$) we found γ values above 0.85 at the vortex shedding frequency f_0 .

In figure 8 the magnitude of the pressure cross spectrum, S_ω , normalized with its maximum value at St_0 , is plotted as

$$S_\omega/S_{\omega\max} = f(St), \quad \Delta\phi = 180^\circ \quad (11a)$$

together with the corresponding power spectrum of the pressure. One may clearly distinguish three easily separable frequency regimes.

(i) Near f_0 the cross spectrum exhibits a peak which is exceptionally narrow indicating a particularly strong periodicity and coherence of the *vortex shedding* mode.

(ii) At twice the vortex shedding frequency, $2f_0$, a second though less clear-cut peak is discernible. This may be taken as a *first harmonic* of the vortex shedding mode which could not be identified in the power spectrum of the pressure. Between these two peaks the cross spectrum drops to very small values indicating that outside these characteristic frequency regimes the underlying 'base' cross spectrum is very small indeed. The first and even a second harmonic can be clearly identified in the velocity power spectra measured by Mercker & Fiedler (1978) in the wake of a wedge (compare with figure 7).

(iii) A third broad hump is seen in figure 8 to arise at frequencies well below f_0 , which also manifests itself in the corresponding power spectrum. Its origin is less obvious than that of the two other peaks.

In the corresponding cross spectra of the axial velocity fluctuations the first regime is even more pronounced than that in the pressure with $S_\omega/S_{\omega\max}$ falling below 0.004 and 0.008 for $St = 0.065$ and 0.185, respectively. This prompted us to plot the related quantity

$$\frac{\gamma}{\gamma_{\max}} = \frac{S_\omega}{S_{\omega\max}} \frac{\tilde{u}_{\omega\max}^2}{\tilde{u}_\omega^2} = f(St); \quad \Delta\phi = 180^\circ, \quad (11b)$$

in figures 6 and 7. Again Roberts' (1973) data at $x = 9D$ fit in quite well. The scatter at higher frequencies renders the identification of a peak at $2f_0$ difficult.

In order to resolve the intrinsic structure of fluctuations in the three frequency regimes separately we will now analyse circumferential correlations for St components at 0.005, 0.135, and 0.27 of both pressure and velocity.

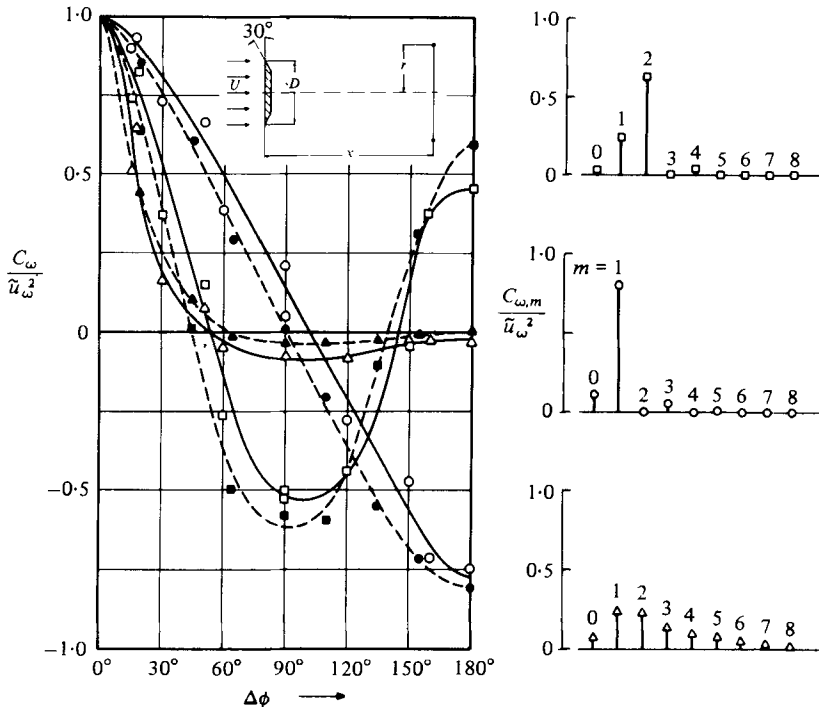


FIGURE 9. Circumferential correlation and azimuthal constituents of narrow band components of the streamwise velocity fluctuations in disk wake at $x = 9D$, $r = 0.83D$. \square , $St = 0.005$; \circ , $St = 0.135$; \triangle , $St = 0.270$; \blacksquare , \bullet , \blacktriangle , corresponding data of Roberts (1973).

7. Azimuthal constituents of large-scale wake structures

We proceed to representation (b) of § 3 by discussing the circumferential variations of

$$C_\omega / \tilde{u}_\omega^2; \quad C_\omega / \tilde{p}_\omega^2 = f(\Delta\phi), \quad St = \text{const.} \tag{12a}$$

as depicted in figures 9–11. Again Roberts' (1973) correlation data at $x = 9D$ are confirmed in figure 9. Our measurements at $x = 3D$ (figure 10) show similar trends for the higher St with a correlation coefficient as high as -0.85 at $St_0 = 0.135$ for $\Delta\phi = 180^\circ$ meaning 85% coherence γ at measuring positions $1.5D$ apart across the wake. That is an even stronger coherence than for signals only $\Delta\phi = 30^\circ$ apart!

With Q_ω effectively zero for all our measurements, the relatively small or zero values of $C_\omega / \tilde{u}_\omega^2$ and hence γ for $\Delta\phi$ around 90° shows up a peculiarity of correlations when dealing with large-scale structures which we want explicitly to mention here.

- (a) Firstly, correlation curves need not look anything like that in figure 1.
- (b) The notion of the degree of correlation or coherence of two signals being indicative of their statistical interdependence is no longer true when γ reaches a number of minimum values at several $\Delta\phi$.

(c) Contrary to what one expects in less ordered turbulent fields, one may find local regions where signal coherence seems to be enhanced with increasing spatial separation. Such apparent anomalies were already observed in the earlier jet studies but are by far more obvious in the wake.

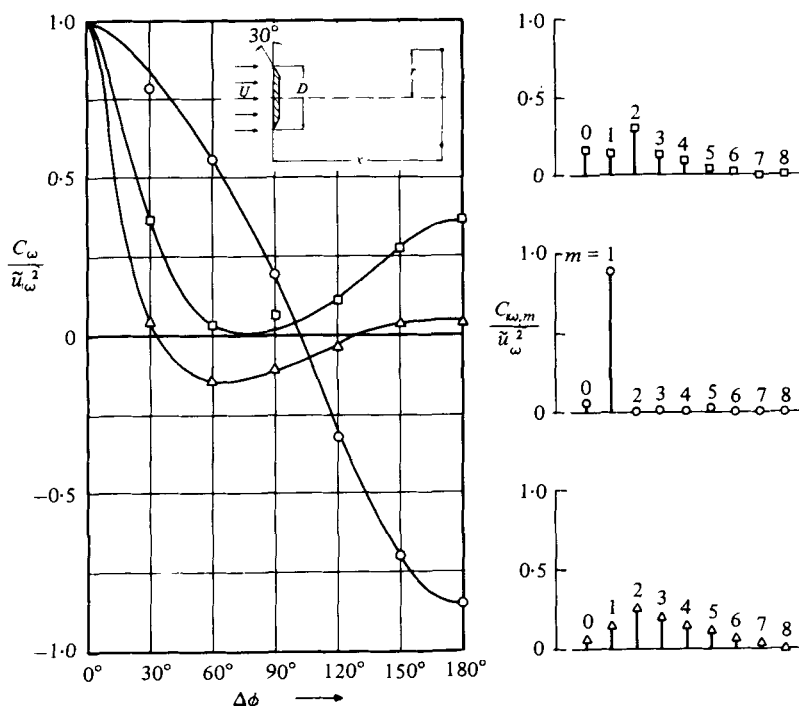


FIGURE 10. Circumferential correlation and azimuthal constituents of narrowband components of the streamwise velocity fluctuations in disk wake at $x = 3D$, $r = 0.75D$. \square , $St = 0.005$; \circ , $St = 0.135$; \triangle , $St = 0.270$.

(d) High negative or correlations alternating in sign are found for probe separations in directions where there is definitely no wave propagation or mean convection ($Q_\omega \cong 0$, $\psi_\omega \cong 0$). These do not define characteristic wavelengths as in a progressive wave field.

(e) The definition of integral length scales l as in equation (4) is totally inappropriate in large-structured fields. Broad-band circumferential correlations, too, would be characterized by the anti-phase features of the strong vortex shedding components thus pretending a negligible l . We cannot follow Prasad & Gupta (1977) either who computed streamwise, lateral, and spanwise scales in plane wakes by simply replacing the upper integral limit infinity by that location where a correlation crosses the abscissa for the first time.

After these more general and qualitative remarks we may discuss the results of the Fourier analysis of the correlation curves in figures 9–11. The coefficients were plotted as

$$C_{\omega,m}/\bar{u}_\omega^2; \quad C_{\omega,m}/\bar{p}_\omega^2 = f(m); \quad St = \text{const.} \quad (13a)$$

for the three frequency regimes defined above.

(i) Not very surprisingly, at $St_0 = 0.135$ it is the $m = 1$ constituent which is, by far, the strongest at any axial position in the velocity as well as in the pressure field. Hardly more than 10% of the fluctuations is contained in any of the other modes. A strong vortex shedding mode was already anticipated in §5 where we have seen an amazing similarity of spectra in the plane and in the axisymmetric wakes (figure 7). We may now conclude that the alternating vortex shedding off the upper and lower

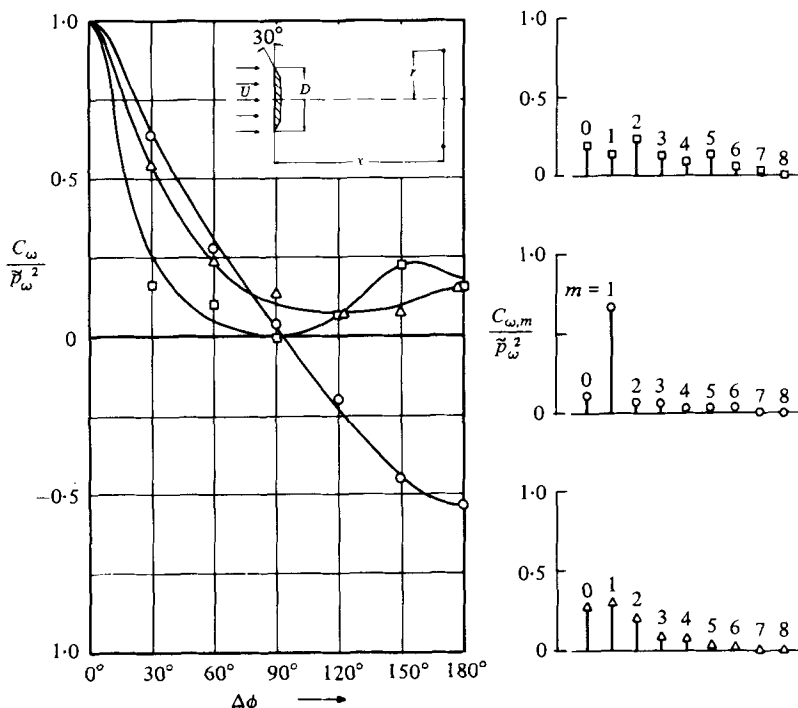


FIGURE 11. Circumferential correlation and azimuthal constituents of narrowband components of pressure fluctuations in disk wake at $x = 3D$, $r = 0.75D$. \square , $St = 0.005$; \circ , $St = 0.135$; \triangle , $St = 0.270$.

parts of a cylinder is paralleled by an anti-phase relationship of signals in the three-dimensional ($3d$) wake. The latter proves the existence of a regular vortex formation which is consistent with the notion of a flapping or fish-tail wiggling type of motion of the whole wake.

Since, contrary to the situation in the $2d$ wake, this flapping motion continuously changes its orientation in a random fashion, the correlation technique favoured in our approach is particularly suited for detecting and quantifying it.

(ii) At high frequencies the correlation curves in figures 9–11 show a more conventional behaviour in that they fall almost monotonically with, at most, minor negative lobes. These trends reflect the presence of a large number of constituents simultaneously. The corresponding plots of $C_{\omega,m}/\bar{u}_\omega^2$ and $C_{\omega,m}/\bar{p}_\omega^2$ indicate only a marginal preference for the $m = 1, 2$ modes with contributions from $m \geq 8$ constituents negligible as in the other frequency regimes.

(iii) In the frequency regime far below St_0 the $m = 1$ constituent is no longer a dominant feature of the axisymmetric wake. Instead, we find the $m = 2$ constituent gaining energy from the others as the wake develops further downstream. At $x = 9D$ (figure 9) more than 60% of the mean-square velocities \bar{u}_ω^2 at $St = 0.005$ contribute to this particular mode which is characterized by an anti-phase relationship at points displaced by $\Delta\phi = \pm 90^\circ$ and by an in-phase relationship for $\Delta\phi = 180^\circ$. The corresponding correlation curve in figure 9 shows this very clearly. It is certainly *not* 'consistent with a slow, random variation in the orientation of a flapping motion' as was erroneously maintained by Roberts (1973).

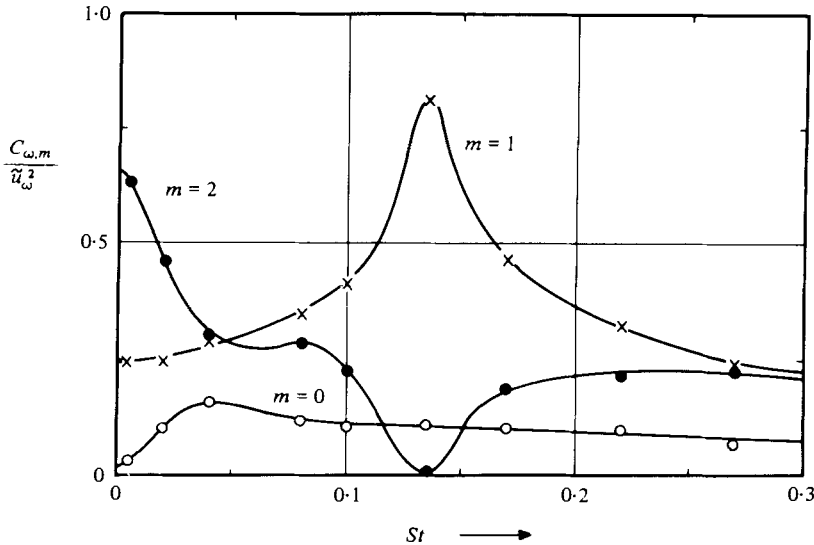


FIGURE 12. Relative strength of individual constituents of wake structures. Correlations and Fourier analyses at $x = 9D$, $r = 0.83D$.

Our complete set of cross spectral analyses in e.g. the plane $x = 9D$, enables correlation curves to be plotted and Fourier analyses performed on them for any arbitrary St . As an interesting variant of representation (c) of § 3 we may now plot

$$\frac{C_{\omega, m}}{\tilde{u}_{\omega}^2} = f(St); \quad m = \text{const.} \quad (13b)$$

with mode number m as a parameter. Figure 12 clearly shows that the $m = 1$ contribution is strongest at $St = St_0$ where the power spectrum \tilde{u}_{ω}^2 itself reaches its maximum (compare with figure 6). This contribution gradually decays on both sides of $St = St_0$ whereas the influence of the $m = 2$ mode increases continuously with decreasing frequency.

Thus the two peaks in the power spectrum of figure 6 do not only correspond to frequency regimes where the coherence of signals is exceptionally high (compare with the γ/γ_{\max} plot in figure 6) but they are also seen to be associated with completely different geometrical structures of the wake. If we assume that all coherent structures in a wake presumably travel downstream at roughly the same speed, we might as well conclude that the two dominant structures, $m = 1$ and 2, must have longitudinal scales or wavelengths Λ_m which differ by, at least, a factor of 10! Obviously, the higher mode $m = 2$ has a much larger axial scale just as if structures of a lower mode are merged in a larger structure of a higher mode on their way downstream.

The $m = 0$ contribution is always smaller than that of the $m = 1$ and 2 constituents and remains almost constant over the whole range of frequencies considered here.

To conclude this paragraph, which covers the main body of results, we plot normalized power spectra with reference to representation (d) of § 3,

$$\frac{\tilde{u}_{\omega, m}^2}{\tilde{u}_{\omega \max}^2} = \frac{C_{\omega, m}}{\tilde{u}_{\omega}^2} \frac{\tilde{u}_{\omega}^2}{\tilde{u}_{\omega \max}^2} = f(St); \quad x, r = \text{const.} \quad (14a)$$

for the individual constituents m . In figure 13 the $\tilde{u}_{\omega, 1}^2$ spectrum is seen to be even more

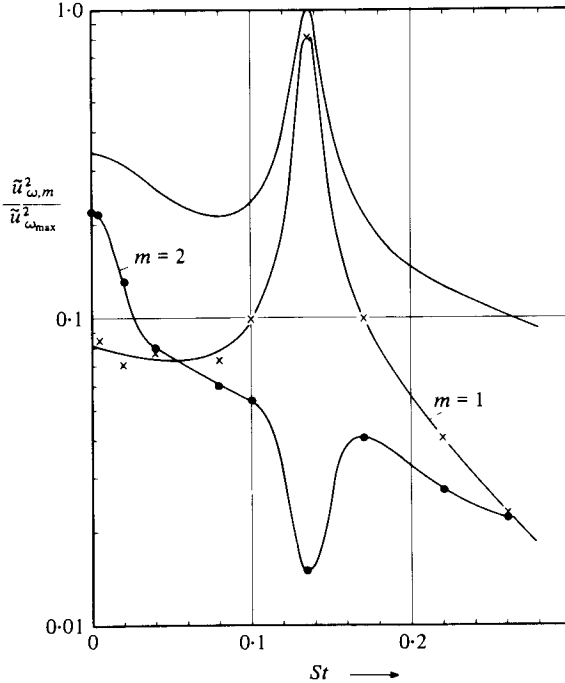


FIGURE 13. Shape of power spectra of dominant azimuthal constituents of wake structures at $x = 9D$, $r = 0.83D$. Upper curve shows overall (unresolved) velocity power spectrum.

narrowband in character than the overall, i.e. unresolved, spectrum \tilde{u}_{ω}^2 . On a logarithmic decibel scale, its peak lies only 1 dB below $\tilde{u}_{\omega_{\max}}^2$ while one octave below or above the vortex shedding frequency $\tilde{u}_{\omega,1}^2$ lies 5 or 6 dB below the respective values of \tilde{u}_{ω}^2 . The $m = 2$ spectrum, on the other hand, peaks about 2 dB below the value of \tilde{u}_{ω}^2 at very low St . The $m = 0$ spectrum would lie at least 2–3 dB below any of the other spectra.

After having separated the predominant vortex shedding ($m = 1$) structure from the rest of the turbulence, we may now return to the periodic phenomena in wake flows. Previous investigators like Hwang & Baldwin (1966) were hardly able to identify the main peak in their velocity spectra. Calvert (1967) says that ‘it has been known for some time that there are periodic phenomena associated with such flows, but that these are not nearly so predominant as in two-dimensional configurations’. Nowhere in the wake was this periodicity sufficiently strong to be identified by either inspection of an oscilloscope trace or smoke observations except at very low Reynolds number.

Our $m = 1$ spectrum in figure 13 proves that our quantitative analysis reveals the periodicity inherent in the wake by removing, very efficiently, the apparent randomness of its orientation in space which has blurred the picture.

8. Comparison with large-scale structures in other flows

In his experiments at $Re = 5 \times 10^4$ in the wake of *cones* with different vertex angles between 0° and 180° (thus including the cylinder and disk) Calvert (1967) found only

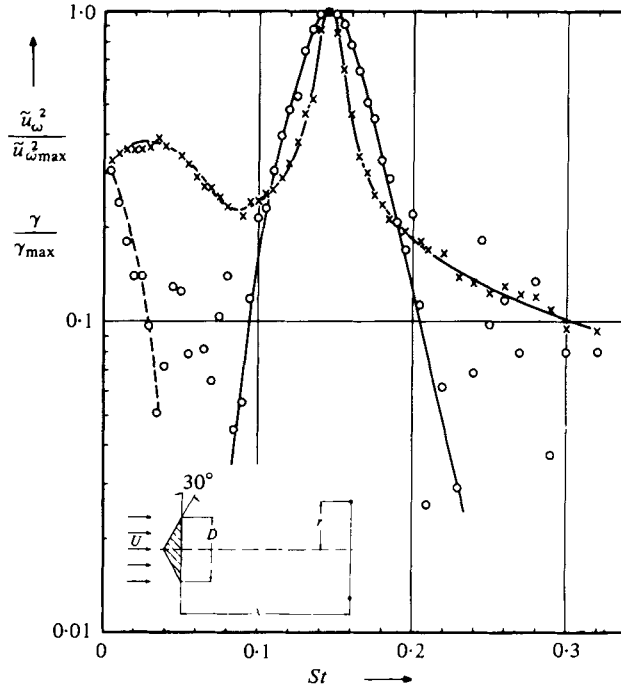


FIGURE 14. Shape of power spectra and coherence spectra of streamwise velocity fluctuations in the wake of a 120° cone. \times , power spectrum at $x = 3D$, $r = 0.75D$; \circ , coherence spectrum, $\Delta\phi = 180^\circ$.

weak periodic motions. Yet he reported typical Strouhal numbers between 0.246 and 0.135, the latter value agreeing very well with our own disk results. It would be interesting to repeat our quantitative analysis with other bluff bodies. So far, we can only compare with the results obtained with a 120° cone. The spectra and cross spectra in figure 14 show only a slight shift of St_0 to 0.145 compared to 0.135 for the disk. This trend confirms earlier observations in the wake of $2d$ bluff bodies. Roshko (1955) found that the shedding frequency scales on the width of the wake which tends to become larger for bluffer bodies of the same frontal area.

The correlation curves for the 120° cone in figure 15 show only minor differences when compared to the disk results in figure 10. Whether or not the wake structures will change more dramatically when cones of smaller vertex angles or the cylinder in a parallel flow are considered remains to be seen. Calvert's (1967) similarity considerations were, in any case, restricted to the mean flow properties and single-point fluctuation measurements only. Likewise, Roshko's (1955) statement that 'the shape or bluntness of the body has no characteristic effect on the wake other than to determine its geometrical and velocity scales' needs further consideration in view of the large-scale structures described in this paper.

The striking periodicity, coherence and regularity which we have identified in our experiments does not seem to exist in the wake formed downstream of central disks located on the centre-line of an *annular jet*. This follows from Durão & Whitelaw (1978), who found the mean flow and single-point turbulent characteristics at 6 jet diameters downstream to be very close to those of a fully developed free jet.

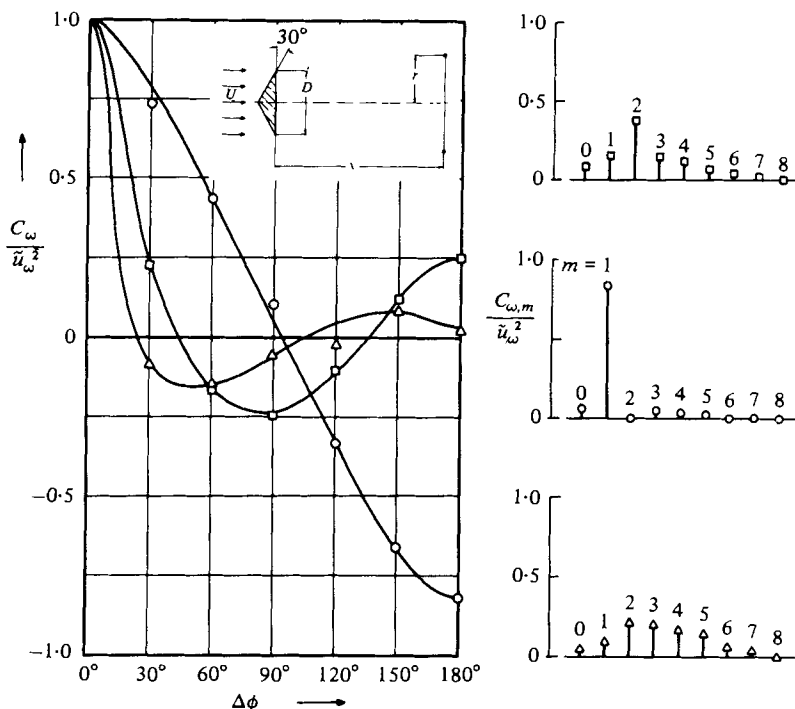


FIGURE 15. Circumferential correlation and azimuthal constituents of velocity fluctuations in the wake of a 120° cone at $x = 3D$, $r = 0.75D$. \square , $St = 0.005$; \circ , $St = 0.145$; \triangle , $St = 0.290$.

The last finding agrees with our own experience with a cylindrical centre-body in a *circular jet* (figure 3). The composition of the large-scale structures by their azimuthal constituents remains more or less unaltered by the presence of the centre body. In particular, the prevailing angular vortex mode ($m = 0$) which presumably does not play an important role in any of the wake flows is only slightly affected by the centre body.

It was already pointed out as another major difference between axisymmetric jet and wake structures that their frequency spectra are considerably broader in the jet than in the wake (compare figures 5 and 6). This also becomes evident when normalized cross spectra are compared (figures 2 and 8).

The most important difference, however, and one of the main results of the present investigation is that the predominant constituents of the wake structures all exhibit completely different spectral distributions with only the $m = 1$ mode peaking at St_0 while the individual jet structures seem to be strongest in a broadly identical range of St (compare figures 4 and 13).

As far as a comparison with the coherent structures in $2d$ wakes is concerned, one would wish to compare the $m = 1$ spectrum of figure 14 with not just the overall $2d$ wake spectrum in figure 7 but with one that has been cleared of those fluctuations which are not strictly anti-phase across the wake. By using the sum and the difference of signals picked up on both sides of the $2d$ wake one might be able to quantify two structural components corresponding to the $m = 0$ and 1 constituents in the axisymmetric wake. Two-point correlations in the near wake of a 90° wedge by Prasad & Gupta (1977) with probe separations in all three directions are considered as a

first step towards a more comprehensive description of $2d$ wake structures. The out-of-phase nature of u fluctuations due to alternate vortex shedding is but weakly indicated in some of their lateral correlations.

Our finding of an almost negligible axisymmetric ($m = 0$) constituent in the wake of a circular disk or cone agrees very nicely with Taneda's (1978) visual observations of the flow past a *sphere*. At all Reynolds numbers Re ranging from 400 to 10^6 he found the sphere wake to never become axisymmetric. At $10^4 < Re < 3.8 \times 10^5$ the sphere wake performs a progressive wave motion in a plane containing the streamwise axis through the centre of the sphere. By means of smoke photographs under 90° from above and from the side like those in his figure 5 Taneda (1978) was able to show that this plane rotates slowly and irregularly about the symmetry axis. The streamwise wavelength equals 4.5 times the sphere diameter, the Strouhal number is $St_0 = 0.2$. Recalling that bluff bodies have lower St_0 according to Roshko (1955) and Calvert (1977), we do not hesitate to directly relate the wave structure in the sphere wake to our $m = 1$ constituent of the disk wake structures.

In this context the visual observations by Pao & Kao (1977) of the sphere wake in a vertically stratified fluid are very informative. Obviously, the stratification provides a preferred direction for the wake oscillations by inhibiting its vertical motions. As a result, at several sphere diameters downstream, a quasi-two-dimensional vortex pattern (of a $m = 1$ structure) is clearly seen to form in the horizontal plane. While a top view of this particular wake reveals all the details of the wake development, a side view shows the complete absence of oscillations in the vertical plane.

Our suggestion of a predominant $m = 1$ structure in the wake of any arbitrary axisymmetric body is also confirmed by Achenbach's (1974) measurements in the near wake of a sphere in a homogeneous uniform flow. By watching oscilloscope traces of hot-wire signals recorded at symmetrical positions $\Delta\phi = 180^\circ$ apart circumferentially, he found the anti-phase situation of the $m = 1$ structure. We cannot follow Achenbach, however, when he associates this as a phase difference of 180° due to a rotation of the wake around the symmetry axis. It is extremely unlikely that a preferred direction was induced by the rotation of his blower generating the flow, simply because it was exactly the same 180° phase difference that was repeatedly measured under completely different upstream conditions like ours. Our view of a random orientation in ϕ of a turbulent structure ($m = 1$) with a built-in anti-phase characteristic of the kind described above is in accordance with that of Taneda (1978).

As the alternating vortex shedding is known to exert a fluctuating lift on a cylinder in a cross flow, one may likewise imagine the sphere or other bluff bodies to be subject to an alternating side force the direction of which is, in general, completely random but always normal to the axis of symmetry. It is pointed out here that no such lateral force will result from any of the other $m \neq 1$ constituents of the wake structures even if they were equally strong.

It may be noted in passing that in the axisymmetric jet case it is the strong $m = 0$ structure that may have an equivalent net effect by causing the forward thrust of the jet to fluctuate thus forming some kind of a feed-back loop. This self-excitation of a jet by a pressure that is in phase over the whole of the nozzle exit plane and which is induced by merely the large coherent structures developing further downstream may well be the reason for the $m = 0$ constituent to be predominant in jet flows.

9. Conclusions

The description of the unsteady processes in the wake flow of axisymmetric bodies represents a long-standing problem of considerable practical relevance. In a note on a paper by Stanton & Marshall (1931) L. Rosenhead put forward some early suggestions about a possible ‘periodic discharge of irregularly shaped ring vortices’. Roshko (1955) deplores the lack of a theory comparable to that of Kármán for the $2d$ vortex street. P. D. Richardson, in a printed discussion of Carmody’s (1964) article, most vividly expressed the need for detailed investigations into the large-scale structures in the wake regions close behind bluff bodies. He already stated that ‘it appears unlikely that a flow possessing distinct and large-scale periodic characteristics can be adequately described and understood in terms of a time-mean flow’. Richardson proposed the use of ‘a suitable hot-wire array to determine the instantaneous direction of flow; the range, distribution, and space-time correlation of this would be very useful information, as would be the local direction correlation also’. He concluded that ‘we have a long way to go in developing techniques of measurement and interpretation before we can be satisfied that we have a sound understanding of the more important details of wake flows’.

We do not claim to have solved the whole problem although our two-point cross spectral analysis and the subsequent spatial resolution of the structures into their azimuthal constituents comes near to what P. D. Richardson, Calvert (1967) and others seem to have called for as a new measuring and analysing technique. Our interpretation of the results is still based on a schematic or symbolic rather than on a physical description of the large-scale structures. The elementary constituents of these structures could be determined in a systematic and quantitative manner. No attempt will be made, however, to speculate about the nature and the origin of the geometrically different structures identified in axisymmetric wakes. It is not at all clear at the moment how these could be associated with ‘horseshoe type vortices’ or ‘double-helix vortex loops’ (Pao & Kao 1977). Nor do we see a possibility to relate our coherent flow structures to any kind of statistical eddy model of the turbulence. We are not even sure whether turbulence researchers would term the large-scale phenomena turbulent as we did.

The proposed technique for describing the large-scale coherent structures in axisymmetric flows may, with some modifications, be applied to other flow configurations, notably those which allow a Fourier analysis in one (or more) distinguished spatial co-ordinate like, e.g., in the spanwise or chordwise directions of $2d$ wakes.

The expansion method is not restricted to ordinary long-time averaged two-point cross correlations. It may equally well be applied to turbulent signals which have been conditioned beforehand such as to reveal details of the structures where this is felt to be essential. This may be necessary when studying, e.g., certain intermittent phenomena in free or bounded shear layers.

Our approach, though generally applicable, will lose its special virtues when dealing with a turbulence field that is something like small-scale homogeneous and isotropic, in which case it would yield not just a few lower-order constituents but a very large number m of constituents of comparable strength and relevance.

Fortunately enough, an amazingly small number of azimuthal constituents representing relatively simple elementary structures or modes suffice to describe the

unsteady flow in axisymmetric jets and wakes. The $m = 0$ and $m = 1$ constituents clearly dominate the initial region of jets at least down to $x = 10D$. The power spectra of both modes are basically similar with their Strouhal frequency peak varying inversely proportional to the downstream distance x . In the wake behind a disk or a cone, on the other hand, it is the $m = 1$ constituent alone that governs the coherent structures at the vortex shedding Strouhal number St_0 whereas the $m = 2$ constituent dominates at very low frequencies.

Whether one can artificially excite the missing $m = 0$ mode in axisymmetric wakes by means of e.g. an externally applied sound field is an open question. Destruction of all the periodic wake phenomena seems to be easily achievable; Fail, Lawford & Eyre (1959) report that 'perforating the plate can eliminate the regular shedding of eddies and reduce the random low-frequency velocity fluctuations'.

In any case, our quantitative analysis of large-scale turbulent structures can serve as a diagnostic tool for investigating the unsteady characteristics of a variety of flow configurations with and without solid boundaries. It is intended, among other things, to apply a similar correlation technique to the coherent structures in turbulent duct flows. Applications to other than axisymmetric flows will follow.

REFERENCES

- ACHENBACH, E. 1974 Vortex shedding from spheres. *J. Fluid Mech.* **62**, 209–221.
- ARMSTRONG, R. R., MICHALKE, A. & FUCHS, H. V. 1977 Coherent structures in jet turbulence and noise. *A.I.A.A. J.* **15**, 1011–1017.
- CALVERT, J. R. 1967 Experiments on the low-speed flow past cones. *J. Fluid Mech.* **27**, 273–289.
- CARMODY, T. 1964 Establishment of the wake behind a disk. *J. Basic Engng* **86**, 869–882.
- DURÃO, D. F. G. & WHITELAW, J. H. 1978 Velocity characteristics of the flow in the near wake of a disk. *J. Fluid Mech.* **85**, 369–385.
- FAIL, R., LAWFOR, J. A. & EYRE, R. C. 1959 Low-speed experiments on the wake characteristics of flat plates normal to an air stream. *Aero. Res. Council. R. & M.* 3120.
- FUCHS, H. V. 1972 Space correlations of the fluctuating pressure in subsonic turbulent jets. *J. Sound Vib.* **23**, 77–99.
- FUCHS, H. V. 1973 Resolution of turbulent jet pressure into azimuthal components. *AGARD Conf. Proc.* no. 131, paper 27.
- FUCHS, H. V., MERCKER, E. & MICHEL, U. 1979 Turbulenzuntersuchungen im Nachlauf einer Kreisscheibe. *Z. Flugwiss.* (To be published).
- FUCHS, H. V. & MICHEL, U. 1977 Experimental evidence of turbulent source coherence effecting jet noise. *A.I.A.A. Paper* **77**, 1348.
- GRANT, H. L. 1958 The large eddies of turbulent motion. *J. Fluid Mech.* **4**, 149–190.
- HWANG, N. H. C. & BALDWIN, L. V. 1966 Decay of turbulence in axisymmetric wakes. *J. Basic Engng* **88**, 261–268.
- KOVASZNAY, L. S. G., KIBENS, V. & BLACKWELDER, R. F. 1970 Large scale motion in the intermittent region of a turbulent boundary layer. *J. Fluid Mech.* **41**, 283–325.
- LAUFER, J., KAPLAN, R. E. & CHU, W. T. 1973 On the generation of jet noise. *AGARD Conf. Proc.* no. 131, paper 21.
- MERCKER, E. & FIEDLER, H. 1978 Eine Blockierungskorrektur für aerodynamische Messungen in geschlossenen Unterschallwindkanälen. *Z. Flugwiss.* **2**.
- MICHALKE, A. & FUCHS, H. V. 1975 On turbulence and noise of an axisymmetric shear flow. *J. Fluid Mech.* **70**, 179–205.
- MICHEL, U. & FUCHS, H. V. 1978 The azimuthal structure of jet pressure near and far fields. *IOA Spring Conf., Camb. Univ.*

- MOORE, C. J. 1977 The role of shear-layer instability waves in jet exhaust noise. *J. Fluid Mech.* **80**, 321–367.
- PAO, H. P. & KAO, T. W. 1977 Vortex structure in the wake of a sphere. *Phys. Fluids* **20**, 187–191.
- PRASAD, J. K. & GUPTA, A. K. 1977 Velocity correlation structure in the turbulent near wake of bluff bodies. *A.I.A.A. J.* **15**, 1569–1574.
- ROBERTS, J. B. 1973 Coherence measurements in an axisymmetric wake. *A.I.A.A. J.* **11**, 1569–1571.
- ROSHKO, A. 1955 On the wake and drag of bluff bodies. *J. Aero. Sci.* **22**, 124–132.
- STANTON, T. E. & MARSHALL, D. 1931 On the eddy system in the wake of flat circular plates in three dimensional flow. *Proc. Roy. Soc. A* **130**, 295.
- SURRY, J. & SURRY, D. 1967 The effect of inclination on the Strouhal number and other wake properties of circular cylinders at subcritical Reynolds numbers. *Univ. Toronto, UTIAS Tech. Note*, no. 116.
- TANEDA, S. 1978 Visual observations of the flow past a sphere at Reynolds numbers between 10^4 and 10^6 . *J. Fluid Mech.* **85**, 187–192.
- TOWNSEND, A. A. 1956 *The Structure of Turbulent Shear Flow*. Cambridge University Press.